Elevated IL-1 Beta Plasma Levels, Altered Platelet Activation and Cardiac Remodeling Lead to Moderately Decreased LV Function in Alzheimer Transgenic Mice After Myocardial Ischemia and Reperfusion

Lili Donner, Simone Gorressen, Jens W. Fischer, Margitta Elvers

Journal of
Cardiovascular Development and Disease

MDPI

Article

Elevated IL-1 Beta Plasma Levels, Altered Platelet Activation and Cardiac Remodeling Lead to Moderately Decreased LV Function in Alzheimer Transgenic Mice After Myocardial Ischemia and Reperfusion

Lili Donner [1], Simone Gorressen [2], Jens W. Fischer [2] and Margitta Elvers [1,*]

[1] Department of Vascular and Endovascular Surgery, Medical Faculty and University Hospital Duesseldorf, Heinrich-Heine-University, 40225 Duesseldorf, Germany; lili.donner@med.uni-duesseldorf.de
[2] Institute of Pharmacology, Medical Faculty and University Hospital Duesseldorf, Heinrich-Heine University, 40225 Duesseldorf, Germany
* Correspondence: margitta.elvers@med.uni-duesseldorf.de

Abstract

Background: Neurodegeneration and dementia are key factors in Alzheimer's disease (AD). The deposition of amyloid-ß into senile plaques in the brain parenchyma and in cerebral vessels known as cerebral amyloid angiopathy (CAA) are the main clinical parameters of AD. Acute myocardial infarction (AMI) and AD share a comparable pathophysiology. However, the underlying mechanisms and the consequences of AMI in AD patients are unclear to date. Methods: AD transgenic APP23 mice were analyzed in experimental AMI using the closed-chest model. Results: APP23 mice displayed significantly decreased left ventricular function as detected by FS/MPI (fractional shortening/myocardial performance index) after 24 h and 3 weeks after ligation of the LAD compared to WT controls. No differences have been observed in infarct and scar size. The analysis of cardiac remodeling after 3 weeks showed an altered composition of the collagen tissue of the scar with elevated tight but reduced fine collagen in APP23 mice. Altered scar formation was accompanied by elevated degranulation of platelets following activation of the collagen receptor GPVI. Conclusions: These results suggest that AD patients are at higher risk for cardiac damage after AMI. This implies the need for a personalized therapy of AMI in AD patients.

Keywords: Alzheimer's disease; platelet activation; myocardial infarction; Aβ; cardiac remodeling

1. Introduction

Alzheimer's disease (AD) is a neurodegenerative disease and the most common form of dementia with a progressive decline in cognitive function [1]. Besides age, the major risk factors are a positive family history, hypertension and hypotension, high cholesterol levels, low levels of physical activity, obesity and the presence of the epsilon 4 allele of the apolipoprotein E gene (APOE4) [2–5].

AD patients present a specific neuropathological profile: the deposition of extracellular amyloid-β (Aβ) into senile plaques and the formation of intracellular neurofibrillary tangles (NFTs) that arise from hyperphosphorylated tau proteins [6]. More than 80% of AD patients develop cerebral amyloid angiopathy (CAA) with Aβ accumulation and aggregation in cerebral vessels [7,8]. In addition, neuroinflammation and blood–brain barrier dysfunction [8] induce neuronal loss and cognitive decline in AD patients.

Received: 2 December 2025
Revised: 15 January 2026
Accepted: 21 January 2026
Published: 26 January 2026

AD and AMI share different pathophysiological hallmarks [9]. AMI is associated with an increased risk of dementia induced by chronic hypo-perfusion of the brain after AMI caused by impaired LV function [10]. Furthermore, the subsequent release of emboli to the brain might be associated with dementia in AMI patients. Thus, AMI is associated with ischemic stroke which in turn increases the risk of dementia [11,12]. Common risk factors such as diabetes mellitus, hypercholesterolemia, hypertension, inflammation and atherosclerosis suggest that AMI and AD may be independent but convergent diseases [13,14]. Different studies suggest that there is a higher risk of dementia in AMI survivors [13].

Platelets are the smallest blood cells and major regulators of hemostasis and thrombosis, but are also a key factor in the pathology of AMI [15–17] and AD [18–26]. Platelet dysfunction is associated with AMI [17,27] and several neurodegenerative diseases such as AD [22,24,28]. Hyper-activation of platelets has been observed in experimental models of AMI [17] and AD [22]. In aged transgenic mice modeling Alzheimer's disease (APP23) with parenchymal plaques and CAA, pre-activated platelets adhere to vascular amyloid-β deposits, leading to cerebral vessel occlusion [21,22]. Thus, platelet activation might be another key element in both AMI and AD.

In this study, we examined the consequences of ischemia and reperfusion injury in APP23 mice. We detected elevated IL-1β plasma levels and platelet degranulation after activation of the collagen receptor GPVI at 21 days after LAD ligation. Furthermore, moderate but significantly decreased LV function was associated with adverse cardiac remodeling while infarct and scar size were not affected.

2. Materials and Methods

2.1. Animals

The transgenic AD mouse model APP23 on a C57BL/6J background was used as described elsewhere [19,29]. APP23 mice first develop individual β-amyloid plaques in the neocortex and in the hippocampus at 6 months of age. The onset of cerebral CAA is at 12 months of age. Degeneration processes can be observed in APP23 mice by the loss of pyramidal neurons in the vicinity of Aβ deposits at the age of 12 month. Hyperphosphorylated microtubule-associated protein tau can also be detected in transgenic brains of APP23 mice. Thus, APP23 mice resemble major features of AD pathology.

Food and water were provided ad libitum. APP23 and non-transgenic littermate (wildtype, WT) mice were fed standard chow. Mice of both sexes were used at an age of 22–25 months, where Aβ pathology was pronounced including amyloid plaques in the parenchym and cerebral vessels. All experiments were performed in accordance with the German Law on the protection of animals and approved by a local ethics committee (LANUV, Essen, Germany, reference number: reference numbers AZ 84-02.04.2013.A473, AZ 81-02.05.40.21.041 and O 86/12).

2.2. Flow Cytometry (Platelet Activation and Annexin-V Binding)

Heparinized whole blood from APP23 and WT littermates was used and diluted in Tyrode's buffer (134 mM NaCl,12 mM $NaHCO_3$, 2.9 mM KCl, 0.34 mM Na_2HPO_4, 20 mM HEPES, 10 mM $MgCl_2$, 5 mM glucose, 0.2 mM $CaCl_2$, pH 7.35) and washed twice. For the analysis of platelet activation, blood samples were mixed with fluorophore-labeled antibodies form Emfret Analytics (P-selectin exposure as marker for degranulation: Wug.E9-FITC, #M130-1; active form of $\alpha_{IIb}\beta_3$ integrin: JON/A-PE, #M023-2, Emfret Analytics, Eibelstadt, Germany) and 2 mM $CaCl_2$ and stimulated with indicated agonists for 15 min at RT. For the analysis of pro-coagulant activity, Annexin-V (#559934, BD Pharmingen, Heidelberg, Germany) binding to cells was determined by flow cytometry.

For determination of Aβ binding to platelets, we used a FITC-labeled Aβ antibody (b-Amyloid antibody (B4)-FITC, #sc-28365 FITC, Santa Cruz Biotechnology, Inc., Dallas, TX, USA) that detects Aβ and amyloid A4 at the surface of platelets.

2.3. Experimental Model of Acute Myocardial Infarction (AMI) and Reperfusion in Mice

A closed-chest model of reperfused myocardial infarction was used in order to reduce surgical trauma and subsequent inflammatory reaction from the intervention as described recently in [17]. Briefly, APP23 and WT littermates were anesthetized with Ketamin (100 mg/kg body weight, Ketaset®, company: Zoetis, Malakoff, France) and Xylazin (10 mg/kg body weight, Xylazin, company: WDT, Ulft, The Netherlands) by a singular intraperitoneal (i.p.) injection before surgery. Euthanasia was performed by cervical dislocation. The left anterior descending artery (LAD) was ligated for 60 min followed by reperfusion for 24 h and 3 weeks as indicated. Coronary occlusion was achieved by gently pulling the applied suture tight until ST-elevation was detected by echocardiography. Thereafter, reperfusion was confirmed by resolution of ST-elevation. After 24 h of reperfusion, hearts were removed and stained with TTC/Evans Blue–solution to stain damaged cardiac tissue of the left ventricle (LV), separated in the area at risk (ischemic area) and the infarcted area. The ratios of the different areas were quantified digitally by video planimetry.

Echocardiography

To determine LV function after AMI, echocardiography was performed at different time points after ischemia and reperfusion (I/R) using Vevo 3100 ultrasound machine (MX400, VisualSonics Inc., Bothell, WA, USA) to measure different parameters, e.g., ejection fraction (%), cardiac output (mL/min), fractional shortening (FS, %), stroke volume (µL) and FS/MPI (myocardial performance index) (%) with corresponding software. In another set of experiments, reperfusion was performed for 3 weeks (21 days).

Cardiac images were acquired using a Vevo 3100 high-resolution ultrasound scanner with 20–46 MHz linear transducer as previously described [30]. Echocardiography was performed under slight mask anesthesia by an inhaled mixture of 1.5–2.0% (*v*/*v*) isoflurane and 100% oxygen. ECGs were obtained with built-in ECG electrode-contact pads. Body temperature was maintained at 36.5–37.5 °C by a heating pad and infrared lamp. All hair was removed from the chest using a chemical hair remover (Veet). Aquasonic 100 gel (Parker Laboratories, Hellendoorn, The Netherlands) was applied to the thorax surface to optimize the visibility of the cardiac chambers. Parasternal long- and short-axis views were acquired. Left ventricular (LV) end-systolic and end-diastolic volumes (ESV and EDV) were acquired in parasternal long-axis view. Ejection fraction was calculated by using the formula EF = (EDV − ESV)/EDV × 100. FS/MPI was calculated using the quotient of FS (Fractional Shortening, Parasternal long axis) and MPI (left ventricular myocardial performance index, PW Doppler Mode, [IVRT + IVCT]/AET). IVCT represents isovolumic contraction time, IVRT represents isovolumic relaxation time, and AET represents aortic ejection time. A single ultrasound session ranged from 15 to 20 min per mouse.

2.4. Determination of IL-1β Plasma Levels

For quantification of IL-1 in the plasma of mice at 24 h post ischemia and reperfusion, heparinized blood was centrifuged 10 min for 650 g to retrieve the plasma. The cytokine amount was measured by IL-1 enzyme-linked immunosorbent assay (ELISA; DuoSet Mouse IL-1β/IL-1F2, R&D systems, Minneapolis, MN, USA) following the manufacturer's protocol.

2.5. Collagen Staining of Cardiac Tissue at 21 Days After Ischemia and Reperfusion

First, scar size was determined by collagen staining 21 days after myocardial infarction by using Gomori's one-step trichrome staining. To this end, heart sections were prepared as mentioned before. The infarct size was expressed as the percentage of the total left ventricular (LV) area. Picrosirius red staining (Morphisto, Frankfurt am Main, Germany) was used for quantification of interstitial collagen deposition and Celestineblue-solution (Sigma, St. Louis, MO, USA) was used to stain nuclei. Interstitial collagen was measured in percent by area fraction.

To distinguish between tight and fine collagen, collagen density was analyzed by polarized light microscopy and birefringence analysis and evaluated by Image J software (Version number V 1.8.0, creator: Wayne Rasband, National Institutes of Health and the Laboratory for Optical and Computational Instrumentation LOCI, University of Wisconsin, Madison, WI, USA) as described recently [17]. Images were captured at 20× magnification. One image was taken in brightfield and one image was taken in polarized light to evaluate thin collagen fibers (collagen type III) in green and dense collagen fibers (collagen type I) in yellow-red in the infarct tissue. Threshold values were chosen for the complete staining and were held constant in the analysis of all images. At least five sections per mouse and group were measured and averaged.

2.6. Statistical Analysis

Data are provided as arithmetic means ± standard error of mean (SEM), statistical analysis was performed using GraphPad Prism Version 9 (Graph Pad Software, Boston, MA, USA). For each experiment, sample size reflects the number of independent biological replicates and is provided in each figure legend. Within this study only independent biological replicates and no technical replicates are shown. Two-tailed unpaired *t*-test or two-way ANOVA with Tukey's multiple comparison test or Sidak's multiple comparison test were used as indicated in the figure legends. A p-value < 0.05 was considered significant (* $p < 0.05$, ** $p < 0.01$, *** $p < 0.001$, **** $p < 0.0001$).

3. Results

3.1. LV Function, Infarct Size, IL-1β Plasma Levels and Platelet Activation in APP23 Mice 24 h After AMI

AD and AMI share common risk factors and might exacerbate disease pathology and all-cause mortality when patients suffer from both diseases. Therefore, we analyzed the consequences of AMI in the AD transgenic mouse line APP23. Experimental ischemia and reperfusion injury was induced in APP23 and WT control mice and LV function was investigated by echocardiography after 24 h of reperfusion (Figure 1A–G). As shown in Figure 1, cardiac output, fractional shortening, ejection fraction, stroke volume, diastolic volume, systolic volume and heart rate were not altered between APP23 and WT control mice (Figure 1A–G) suggesting unaltered LV function in APP23 mice compared to controls.

Furthermore, infarct size was not different between APP23 and WT controls (Figure 2A). However, we detected elevated IL-1β but reduced IL-6 plasma levels in AD transgenic mice suggesting altered inflammation in these mice (Figure 2B,C). Flow cytometry was used to analyze platelet pro-coagulant activity by Annexin-V binding of platelets (Figure 2D) and platelet activation by determination of active integrin $\alpha_{IIb}\beta_3$ and P-selectin exposure (marker for degranulation). As shown in Figure 2E,F, no differences were observed between APP23 and WT control mice (Figure 2E,F).

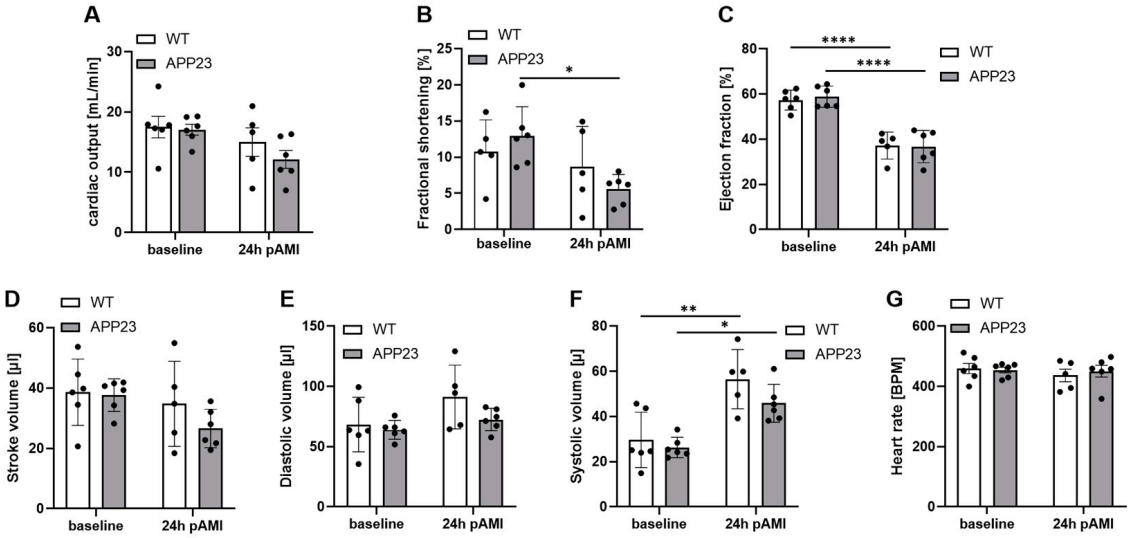

Figure 1. No differences in left ventricular function in APP23 mice 24 h post AMI. Echocardiographic analysis of cardiac function by determination of (**A**) cardiac output (mL/min.), (**B**) fractional shortening (%), (**C**) ejection fraction (%), (**D**) stroke volume (µL), (**E**) diastolic volume (µL), (**F**) systolic volume (µL) and (**G**) heart rate (BPM). Baseline vs. 24 h after ischemia and reperfusion are shown. Bar graphs indicate mean values ± SEM. Statistical analyses were performed using a two-way ANOVA with Sidak's multiple comparison test (**A**,**G**) or with Tukey's multiple comparison test (**B**–**G**). N = 5–6. * $p < 0.05$; ** $p < 0.01$; **** $p < 0.0001$. BPM = beats per minute.

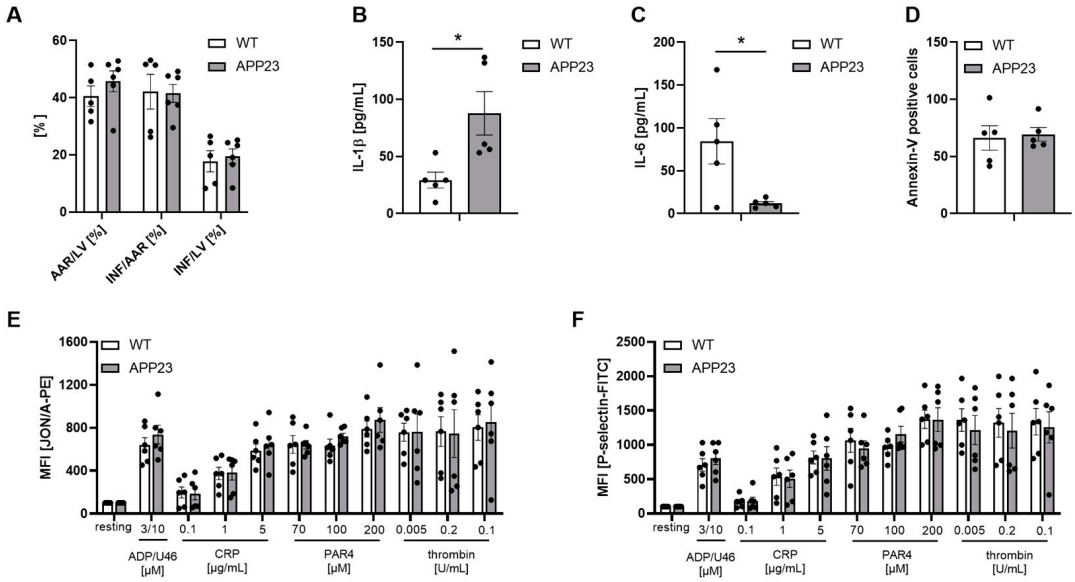

Figure 2. Unaltered infarct size and platelet activation but altered acute phase cytokine plasma levels in APP23 mice 24 h after ischemia and reperfusion. (**A**) Quantitative analysis of infarct size as the percentage of area at risk (% Inf/AAR, left panel) 24 h post AMI. (**B**) IL-1β and (**C**) IL-6 plasma levels in WT vs. APP23 mice 24 h post ischemia and reperfusion (**D**–**F**). Flow cytometry was used to determine Annexin V binding to platelets as a marker for pro-coagulant activity (**D**) and platelet activation following stimulation of platelets with indicated agonists. Platelet activation was detected by measuring active integrin $\alpha_{IIb}\beta_3$ using the JON/A antibody (**E**) and by determination of P-selectin exposure at the platelet membrane as marker for degranulation (**F**). Results are shown as MFI (mean fluorescence intensity). Bar graphs indicate mean values ± SEM. Statistical analyses were performed using a two-way ANOVA with Tukey's multiple comparison test (**A**) or Sidak's multiple comparison test (**E**,**F**) or a two-tailed unpaired *t*-test (**B**–**D**). N = 5–6. * $p < 0.05$; ADP = adenosinediphosphate; U46 = thromboxane analog; PAR4 = PAR4 peptide, activates the thrombin receptor PAR4; CRP = collagen-related peptide, activates the collagen receptor GPVI.

Moreover, blood cell counts such as the number of red and white blood cells and platelets were not altered, neither 24 h nor 21 days post ischemia and reperfusion (Supplementary Figure S1).

3.2. Moderately Reduced LV Function After 21 Days Following Ischemia and Reperfusion Injury in APP23 Mice

The analysis of LV function after 3 weeks of ischemia and reperfusion in APP23 mice revealed reduced FS/MPI while no alterations were detected with regard to cardiac output, fractional shortening, ejection fraction and stroke volume as analyzed by echocardiography (Figure 3). Moreover, diastolic volume and systolic volume were unaltered between APP23 and WT control mice. Thus, moderately decreased LV function in APP23 mice after 21 days post ischemia and reperfusion revealed prolonged cardiac dysfunction in AD transgenic mice after AMI.

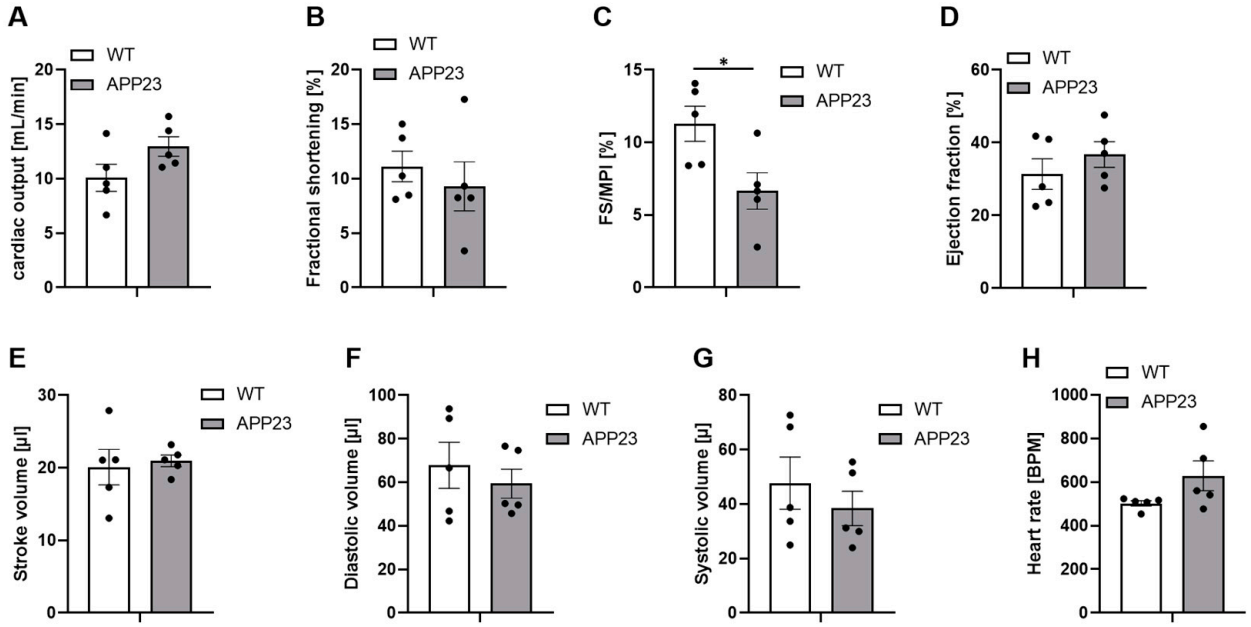

Figure 3. Moderately reduced FS/MPI in APP23 mice 21 days post ischemia and reperfusion. Echocardiographic analysis of cardiac function by determination of (**A**) cardiac output (mL/min.), (**B**) fractional shortening (%), (**C**) FS/MPI (%), (**D**) ejection fraction (%), (**E**) stroke volume (µL), (**F**) diastolic volume (µL), (**G**) systolic volume (µL) and (**H**) heart rate (BPM). WT vs. APP23 mice 21 d after ischemia and reperfusion are shown. Bar graphs indicate mean values ± SEM. Statistical analyses were performed using a two-tailed unpaired *t*-test. N = 5. * $p < 0.05$. FS/MPI = fractional shortening/myocardial performance index; BPM = beats per minute.

3.3. Altered Scar Formation with Elevated Tight but Reduced Fine Collagen in APP23 Mice Did Not Result in Different Scar Size

No differences in scar size were detected in AD transgenic mice (Figure 4A,B) 21 days after ischemia and reperfusion injury. In addition, interstitial collagen was not altered (Figure 4C). In contrast, cardiac remodeling as indicated by collagen composition of the scar revealed differences in the level of tight and fine collagen. In detail, increased levels of tight collagen but reduced fine collagen have been detected in APP23 compared to WT control mice (Figure 4D,E). Thus, differences in the collagen composition might change scar quality but not scar size leading to reduced LV function in AD transgenic mice.

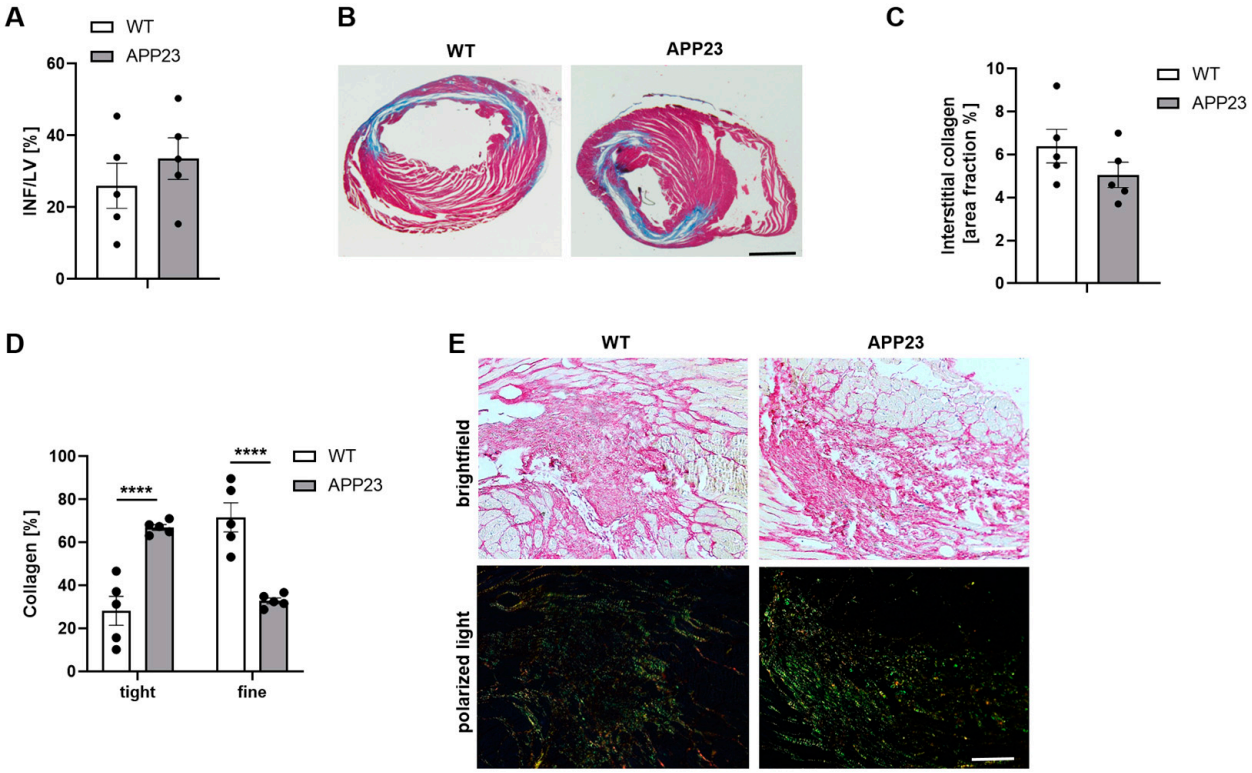

Figure 4. Unaltered scar size but different scar quality at 21 days post AMI. Quantification (**A**) and representative images of scar size (**B**) using Gomori's trichrome staining 21 days post AMI. Infarcted area is stained in blue and healthy tissue is stained in red. Data are presented as means ± SEM. (**C**) Quantification of sirius-red staining of interstitial collagen in the remote zone of APP23 mice after 21 days of reperfusion compared to WT controls. Analysis of collagen composition (**D**) and representative images of sirius-red staining (**E**) of APP23 mice after 21 days of reperfusion compared to their littermate controls. In bright field microscopy of the LV after AMI, the cytoplasm is stained in yellow and collagen is stained in red. Polarized light microscopy was used to identify fine collagen fibers (collagen type III) in green and dense collagen fibers (collagen type I) in yellow-red. Scale bar = 2 mm (**B**), 100 µm (**E**). Bar graph depicts mean values ± SEM. Statistical analyses were performed using a two-tailed unpaired *t*-test (**A**,**C**) or a two-way ANOVA with Sidak's multiple comparison test (**D**). N = 5. **** $p < 0.0001$.

3.4. Alterations in Platelet Activation in APP23 Mice After AMI Suggest an Impact of Platelets in Cardiac Damage

Next, we analyzed platelet activation since platelets play a role in AMI and AD. As shown in Figure 5, integrin $\alpha_{IIb}\beta_3$ activation as reflected by JON/A binding to platelets revealed no differences between groups (Figure 5A). In contrast, P-selectin exposure at the platelet surface as a marker for platelet degranulation was elevated in response to collagen-related peptides that activate the major collagen receptor GPVI at the platelet surface. Moreover, thrombin stimulation of platelets resulted in reduced P-selectin exposure of platelets from APP23 mice (Figure 5B). Since platelets and, in particular, the collagen receptor GPVI are known to modulate inflammation and cardiac remodeling after AMI—at least in mice—[16,17], the results point to an impact of platelets in scar formation and cardiac function in AD transgenic mice as reflected by altered levels of tight and fine collagen in the scar and reduced FS/MPI as detected by echocardiography.

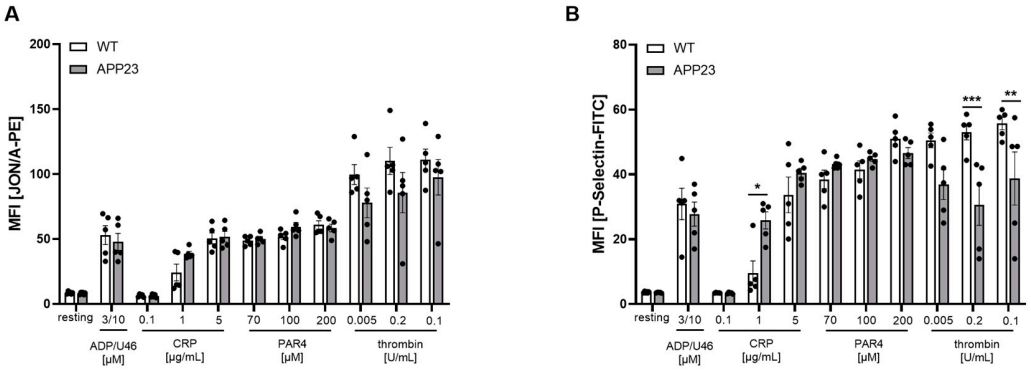

Figure 5. Flow cytometric analysis revealed enhanced platelet activation in response to GPVI in APP23 mice at 21 days post AMI. (**A**) Active integrin (JON/A-PE binding to integrin $\alpha_{IIb}\beta_3$) and (**B**) platelet degranulation (P-selectin-PE) under resting and activated conditions were determined by flow cytometry using whole blood from APP23 and WT control mice. Different agonists were used to activate different signaling pathways in platelets. Data are represented as MFI. Bar graphs indicate mean values ± SEM. Statistical analyses were performed using a two-way ANOVA with Sidak's multiple comparison test. * $p < 0.05$; ** $p < 0.01$; *** $p < 0.001$. ADP = adenosinediphosphate; U46 = thromboxane analog; PAR4 = PAR4 peptide, activates the thrombin receptor PAR4; CRP = collagen-related peptide, activates the collagen receptor GPVI; MFI, mean fluorescence intensity. N = 5.

4. Discussion

In recent years, an association of AD and heart failure including chronic and acute events such as AMI has been described. The multitude of published data focuses on the effects of cardiovascular disease on dementia including AD. Here, we provide evidence that mice with AD show impaired LV function and altered scar formation after ischemia and reperfusion injury. Thus, this is the first study to analyze the effects of AD including amyloid pathology in cerebral vessels and the brain parenchyma and how this affects cardiac damage after AMI, at least in mice. However, elevated IL-1β plasma levels and altered cardiac remodeling leads to only moderately decreased LV function as detected by reduced FS/MPI.

After AMI, echocardiography revealed only moderately reduced LV function in APP23 mice compared to controls after 21 days post ischemia and reperfusion injury. In detail, we detected significantly reduced FS/MPI whereas no differences were observed in cardiac output, fractional shortening, and ejection fraction and stroke volume (Figure 3). However, it has been shown that the FS/MPI ratio is the best noninvasive index of LV function in mice [31]. Moreover, MPI strongly correlates with dP/dt_{max} over a range of hemodynamic conditions in mice with the best correlation of FS/MPI with dP/dt_{max}. Thus, our results clearly suggest that AD pathology is associated with moderately decreased LV function after AMI.

Published data describes a relationship between heart failure and AD. Therefore, heart failure as reflected by reduced cardiac output and neuro-hormonal activation leads to reduced cerebral blood flow and hypoxia in the brain. Hypoxia results in tau hyperphosphorylation, amyloid precursor protein cleavage, dysfunction of the neurovascular unit and oxidative stress. These cellular responses then in turn induce the formation of neurofibrillary tangles and amyloid-β plaques, impaired amyloid-β clearance and inflammation, including dysfunction of microglia and thus AD [32]. Thorp and colleagues found an association of AMI and vascular dementia with inflammation induced by ischemia and reperfusion injury leading to neurovascular injury [14]. The risk of vascular dementia is increased in survivors of AMI. The authors found that this association was even stronger in

patients with stroke. However, Sundboll and colleagues were not able to provide evidence for an increased risk of AD in patients with AMI [13].

Blood levels of Aβ40 play a role in the survival rate of AMI patients. In detail, measuring the blood levels of Aβ40 in patients with coronary heart disease may identify patients with high risk of cardiovascular death [33]. Thus, Aβ40 might serve as a biomarker to identify patients with cardiovascular disease and increased risk of death.

An interplay of cardiovascular risk factors and an increased risk of cognitive impairment and AD have been described by different groups. To this end, atherosclerosis plays a key role in this interplay including endothelial dysfunction and cerebral hypo-perfusion. Moreover, diabetes mellitus [34], arterial hypertension [35] and dyslipidemia [36] are risk factors for cardiovascular disease and cognitive impairment [37]. Different patient studies support this interplay of cardiovascular disease and AD. The prospective Rotterdam Study provides evidence for a two-threefold higher risk of developing AD in patients with severe atherosclerosis [38]. In a primary care patients study, this data was confirmed because coronary artery disease (CAD) has an effect on mild cognitive impairment (MCI) in patients with AD [39].

Interestingly, carriers of the ApoE4 allele have been shown to present a more marked association between CAD and neuropathological lesion of AD than patients who do not present this allele [9]. Thus, ApoE might affect both CAD and AD neuropathology. However, testing for ApoE cannot predict the development of AD in patients but might be useful to identify subjects at risk. Liu and colleagues found that AMI and AD share a comparable pathophysiology that may be mediated by certain hub genes. They identified the BCL6 gene to be essential for developing AMI and AD.

Recently, a retrospective cohort study provides evidence for patients with pre-existing AD to have a poor prognosis when they develop AMI because they showed a high rate of major adverse cardiovascular events (MACE) and all-cause mortality. Patients with AD were older, more likely to be female, and had a greater burden of individual comorbidities and multi-morbidity. AD patients who were selected to undergo invasive management experienced reduce MACE and all-cause mortality compared to those managed conservatively. Thus, future research should identify patients who might benefit from invasive management. Furthermore, individualized multidisciplinary decision-making is key to provide the best therapy for AD patients with AMI.

Differences in the inflammatory response after AMI as shown here by altered IL-1 and IL-6 plasma levels of APP23 and control mice further suggest a patient-based therapy concept (Figure 2). This idea is further supported by differences in platelet activation in APP23 mice. While no major differences have been observed after 24 h (Figure 2), we detected differences in P-selectin exposure of platelets after 3 weeks of I/R (Figure 5). In detail, elevated P-selectin exposure has been observed after intermediate concentrations of CRP suggesting elevated GPVI activation while the incubation of platelets with thrombin leads to reduced platelet activation at low and intermediate concentrations of the agonist. Thus, not only the inflammatory response but also platelet activation is dysregulated in APP23 mice compared to WT controls after I/R.

One possible link between AD and AMI may be platelets and their altered activation profile in both diseases. Platelets show a hyperactive profile in AD [22] and affect CAA [19], at least in mice. In AMI, platelet activation is altered as well. In thrombocytopenic mice, a reduced inflammatory response was observed after ischemia and reperfusion injury [17]. Moreover, platelets actively contribute to cardiac remodeling and scar formation and thus affect infarct size and heart function [16,17]. Importantly, the major collagen receptor GPVI might play a dominant role in the abovementioned cellular responses. Thus, it is not surprising that increased platelet activation in APP23 mice was detected mainly following

GPVI activation using platelets from mice at 21 days post ischemia and reperfusion. Therefore, we believe that platelets might be one important player in the relationship between AD and AMI.

5. Conclusions

Taken together, AMI in AD transgenic mice leads to dysregulated levels of acute phase cytokines in plasma, increased platelet activation in response to GPVI and altered cardiac remodeling at 21 days post ischemia and reperfusion, resulting in moderately decreased LV function in APP23 mice after 21 days post I/R. With regard to recently published data from AD patients with AMI, further research is important to further investigate the relationship of both diseases and to conduct a personalized therapy for patients at high risk of cardiovascular death.

Supplementary Materials: The following supporting information can be downloaded at: https://www.mdpi.com/article/10.3390/jcdd13020064/s1, Figure S1: Analysis of blood cell counts of WT and APP23 mice after AMI.

Author Contributions: M.E. and J.W.F. designed the study. L.D. and S.G. performed experiments. M.E., J.W.F. and L.D. analyzed and interpreted data. M.E. wrote the manuscript with all authors providing feedback. All authors have read and agreed to the published version of the manuscript.

Funding: This research was funded by a grant from the German Research Foundation (Deutsche Forschungsgemeinschaft, DFG), project number 392381697 to M.E.

Institutional Review Board Statement: All experiments were performed in accordance with the German Law on the protection of animals and approved by a local ethics committee (LANUV, North-Rhine-Westphalia, Germany, reference number: reference numbers AZ 84-02.04.2013.A473 (approval date: 4 February 2014), AZ 84-02.05.20.12.284 (approval date 14 November 2012), AZ 81-02.05.40.16.073 (approval date 30 November 2016) and O 86/12 (approval date 29 October 2012).

Informed Consent Statement: Not applicable.

Data Availability Statement: The original contributions presented in this study are included in the article/Supplementary Materials. Further inquiries can be directed to the corresponding author.

Acknowledgments: We thank Martina Spelleken and Dominik Semmler for providing outstanding technical assistance.

Conflicts of Interest: The authors declare no conflicts of interest.

Abbreviations

The following abbreviations are used in this manuscript:

AD	Alzheimer's disease
ADP	adenosinediphosphate
AMI	Acute Myocardial Infarction
Aβ	amyloid-β
APOE4	apolipoprotein E 4 gene
CAA	Cerebral Amyloid Angiopathy
CRP	collagen-related peptide
FS	fractional shortening
LAD	left anterior descending artery
LV	left ventricle
MACE	major adverse cardiovascular events
MFI	mean fluorescence intensity
MPI	myocardial performance index
WT	wildtype

References

1. Clarfield, A.M. The decreasing prevalence of reversible dementias: An updated meta-analysis. *Arch. Intern. Med.* **2003**, *163*, 2219–2229. [CrossRef]
2. Huang, W.; Qiu, C.; von Strauss, E.; Winblad, B.; Fratiglioni, L. APOE genotype, family history of dementia, and Alzheimer disease risk: A 6-year follow-up study. *Arch. Neurol.* **2004**, *61*, 1930–1934. [CrossRef]
3. Kivipelto, M.; Helkala, E.L.; Laakso, M.P.; Hänninen, T.; Hallikainen, M.; Alhainen, K.; Soininen, H.; Tuomilehto, J.; Nissinen, A. Midlife vascular risk factors and Alzheimer's disease in later life: Longitudinal, population based study. *BMJ* **2001**, *322*, 1447–1451. [CrossRef]
4. Kivipelto, M.; Ngandu, T.; Fratiglioni, L.; Viitanen, M.; Kåreholt, I.; Winblad, B.; Helkala, E.L.; Tuomilehto, J.; Soininen, H.; Nissinen, A. Obesity and vascular risk factors at midlife and the risk of dementia and Alzheimer disease. *Arch. Neurol.* **2005**, *62*, 1556–1560. [CrossRef]
5. Wallin, K.; Boström, G.; Kivipelto, M.; Gustafson, Y. Risk factors for incident dementia in the very old. *Int. Psychogeriatr.* **2013**, *25*, 1135–1143. [CrossRef]
6. Long, J.M.; Holtzman, D.M. Alzheimer Disease: An Update on Pathobiology and Treatment Strategies. *Cell* **2019**, *179*, 312–339. [CrossRef]
7. Selkoe, D.J. Alzheimer's disease. *Cold Spring Harb. Perspect. Biol.* **2011**, *3*, a004457. [CrossRef]
8. Thal, D.R.; Griffin, W.S.; de Vos, R.A.; Ghebremedhin, E. Cerebral amyloid angiopathy and its relationship to Alzheimer's disease. *Acta Neuropathol.* **2008**, *115*, 599–609. [CrossRef]
9. Liu, C.; Pan, F.; Sun, Z.; Chen, Z.; Wang, J. Exploring the pathogenesis and key genes associated of acute myocardial infarction complicated with Alzheimer's disease. *Sci. Rep.* **2024**, *14*, 1449. [CrossRef]
10. Zuccalà, G.; Onder, G.; Pedone, C.; Carosella, L.; Pahor, M.; Bernabei, R.; Cocchi, A. Hypotension and cognitive impairment: Selective association in patients with heart failure. *Neurology* **2001**, *57*, 1986–1992. [CrossRef]
11. Corraini, P.; Henderson, V.W.; Ording, A.G.; Pedersen, L.; Horváth-Puhó, E.; Sørensen, H.T. Long-Term Risk of Dementia Among Survivors of Ischemic or Hemorrhagic Stroke. *Stroke* **2017**, *48*, 180–186. [CrossRef]
12. Sundbøll, J.; Horváth-Puhó, E.; Schmidt, M.; Pedersen, L.; Henderson, V.W.; Bøtker, H.E.; Sørensen, H.T. Long-Term Risk of Stroke in Myocardial Infarction Survivors: Thirty-Year Population-Based Cohort Study. *Stroke* **2016**, *47*, 1727–1733. [CrossRef]
13. Sundbøll, J.; Horváth-Puhó, E.; Adelborg, K.; Schmidt, M.; Pedersen, L.; Bøtker, H.E.; Henderson, V.W.; Sørensen, H.T. Higher Risk of Vascular Dementia in Myocardial Infarction Survivors. *Circulation* **2018**, *137*, 567–577. [CrossRef]
14. Thorp, E.B.; Flanagan, M.E.; Popko, B.; DeBerge, M. Resolving inflammatory links between myocardial infarction and vascular dementia. *Semin. Immunol.* **2022**, *59*, 101600. [CrossRef]
15. Krott, K.J.; Reusswig, F.; Dille, M.; Krüger, E.; Gorressen, S.; Karray, S.; Polzin, A.; Kelm, M.; Fischer, J.W.; Elvers, M. Platelets Induce Cell Apoptosis of Cardiac Cells via FasL after Acute Myocardial Infarction. *Biomedicines* **2024**, *12*, 1077. [CrossRef]
16. Reusswig, F.; Dille, M.; Krüger, E.; Ortscheid, J.; Feige, T.; Gorressen, S.; Fischer, J.W.; Elvers, M. Platelets modulate cardiac remodeling via the collagen receptor GPVI after acute myocardial infarction. *Front. Immunol.* **2023**, *14*, 1275788. [CrossRef]
17. Reusswig, F.; Polzin, A.; Klier, M.; Dille, M.A.; Ayhan, A.; Benkhoff, M.; Lersch, C.; Prinz, A.; Gorressen, S.; Fischer, J.W.; et al. Only Acute but Not Chronic Thrombocytopenia Protects Mice against Left Ventricular Dysfunction after Acute Myocardial Infarction. *Cells* **2022**, *11*, 3500. [CrossRef]
18. Chen, M.; Inestrosa, N.C.; Ross, G.S.; Fernandez, H.L. Platelets are the primary source of amyloid beta-peptide in human blood. *Biochem. Biophys. Res. Commun.* **1995**, *213*, 96–103. [CrossRef]
19. Donner, L.; Falker, K.; Gremer, L.; Klinker, S.; Pagani, G.; Ljungberg, L.U.; Lothmann, K.; Rizzi, F.; Schaller, M.; Gohlke, H.; et al. Platelets contribute to amyloid-beta aggregation in cerebral vessels through integrin alphaIIbbeta3-induced outside-in signaling and clusterin release. *Sci. Signal.* **2016**, *9*, ra52. [CrossRef]
20. Donner, L.; Toska, L.M.; Krüger, I.; Gröniger, S.; Barroso, R.; Burleigh, A.; Mezzano, D.; Pfeiler, S.; Kelm, M.; Gerdes, N.; et al. The collagen receptor glycoprotein VI promotes platelet-mediated aggregation of β-amyloid. *Sci. Signal.* **2020**, *13*, eaba9872. [CrossRef]
21. Gowert, N.S.; Donner, L.; Chatterjee, M.; Eisele, Y.S.; Towhid, S.T.; Munzer, P.; Walker, B.; Ogorek, I.; Borst, O.; Grandoch, M.; et al. Blood platelets in the progression of Alzheimer's disease. *PLoS ONE* **2014**, *9*, e90523. [CrossRef]
22. Jarre, A.; Gowert, N.S.; Donner, L.; Munzer, P.; Klier, M.; Borst, O.; Schaller, M.; Lang, F.; Korth, C.; Elvers, M. Pre-activated blood platelets and a pro-thrombotic phenotype in APP23 mice modeling Alzheimer's disease. *Cell. Signal.* **2014**, *26*, 2040–2050. [CrossRef]
23. Koupenova, M.; Clancy, L.; Corkrey, H.A.; Freedman, J.E. Circulating Platelets as Mediators of Immunity, Inflammation, and Thrombosis. *Circ. Res.* **2018**, *122*, 337–351. [CrossRef]
24. Leiter, O.; Walker, T.L. Platelets in Neurodegenerative Conditions-Friend or Foe? *Front. Immunol.* **2020**, *11*, 747. [CrossRef]
25. Li, Q.X.; Whyte, S.; Tanner, J.E.; Evin, G.; Beyreuther, K.; Masters, C.L. Secretion of Alzheimer's disease Abeta amyloid peptide by activated human platelets. *Lab. Investig.* **1998**, *78*, 461–469.

26. Wolska, N.; Celikag, M.; Failla, A.V.; Tarafdar, A.; Renné, T.; Torti, M.; Canobbio, I.; Pula, G. Human platelets release amyloid peptides β(1-40) and β(1-42) in response to haemostatic, immune, and hypoxic stimuli. *Res. Pract. Thromb. Haemost.* **2023**, *7*, 100154. [CrossRef]
27. Michaels, A.D.; Gibson, C.M.; Barron, H.V. Microvascular dysfunction in acute myocardial infarction: Focus on the roles of platelet and inflammatory mediators in the no-reflow phenomenon. *Am. J. Cardiol.* **2000**, *85*, 50b–60b. [CrossRef]
28. Beura, S.K.; Panigrahi, A.R.; Yadav, P.; Singh, S.K. Role of platelet in Parkinson's disease: Insights into pathophysiology & theranostic solutions. *Ageing Res. Rev.* **2022**, *80*, 101681. [CrossRef] [PubMed]
29. Sturchler-Pierrat, C.; Abramowski, D.; Duke, M.; Wiederhold, K.H.; Mistl, C.; Rothacher, S.; Ledermann, B.; Bürki, K.; Frey, P.; Paganetti, P.A.; et al. Two amyloid precursor protein transgenic mouse models with Alzheimer disease-like pathology. *Proc. Natl. Acad. Sci. USA* **1997**, *94*, 13287–13292. [CrossRef] [PubMed]
30. Heinen, A.; Raupach, A.; Behmenburg, F.; Hölscher, N.; Flögel, U.; Kelm, M.; Kaisers, W.; Nederlof, R.; Huhn, R.; Gödecke, A. Echocardiographic Analysis of Cardiac Function after Infarction in Mice: Validation of Single-Plane Long-Axis View Measurements and the Bi-Plane Simpson Method. *Ultrasound Med. Biol.* **2018**, *44*, 1544–1555. [CrossRef]
31. Broberg, C.S.; Pantely, G.A.; Barber, B.J.; Mack, G.K.; Lee, K.; Thigpen, T.; Davis, L.E.; Sahn, D.; Hohimer, A.R. Validation of the myocardial performance index by echocardiography in mice: A noninvasive measure of left ventricular function. *J. Am. Soc. Echocardiogr.* **2003**, *16*, 814–823. [CrossRef]
32. Cermakova, P.; Eriksdotter, M.; Lund, L.H.; Winblad, B.; Religa, P.; Religa, D. Heart failure and Alzheimer's disease. *J. Intern. Med.* **2015**, *277*, 406–425. [CrossRef] [PubMed]
33. Stamatelopoulos, K.; Sibbing, D.; Rallidis, L.S.; Georgiopoulos, G.; Stakos, D.; Braun, S.; Gatsiou, A.; Sopova, K.; Kotakos, C.; Varounis, C.; et al. Amyloid-beta (1-40) and the risk of death from cardiovascular causes in patients with coronary heart disease. *J. Am. Coll. Cardiol.* **2015**, *65*, 904–916. [CrossRef]
34. Craft, S.; Asthana, S.; Schellenberg, G.; Cherrier, M.; Baker, L.D.; Newcomer, J.; Plymate, S.; Latendresse, S.; Petrova, A.; Raskind, M.; et al. Insulin metabolism in Alzheimer's disease differs according to apolipoprotein E genotype and gender. *Neuroendocrinology* **1999**, *70*, 146–152. [CrossRef]
35. Guo, Z.; Fratiglioni, L.; Viitanen, M.; Lannfelt, L.; Basun, H.; Fastbom, J.; Winblad, B. Apolipoprotein E genotypes and the incidence of Alzheimer's disease among persons aged 75 years and older: Variation by use of antihypertensive medication? *Am. J. Epidemiol.* **2001**, *153*, 225–231. [CrossRef] [PubMed]
36. Evans, R.M.; Hui, S.; Perkins, A.; Lahiri, D.K.; Poirier, J.; Farlow, M.R. Cholesterol and APOE genotype interact to influence Alzheimer disease progression. *Neurology* **2004**, *62*, 1869–1871. [CrossRef] [PubMed]
37. Tini, G.; Scagliola, R.; Monacelli, F.; La Malfa, G.; Porto, I.; Brunelli, C.; Rosa, G.M. Alzheimer's Disease and Cardiovascular Disease: A Particular Association. *Cardiol. Res. Pract.* **2020**, *2020*, 2617970. [CrossRef]
38. Breteler, M.M.; Claus, J.J.; Grobbee, D.E.; Hofman, A. Cardiovascular disease and distribution of cognitive function in elderly people: The Rotterdam Study. *BMJ* **1994**, *308*, 1604–1608. [CrossRef]
39. Bleckwenn, M.; Kleineidam, L.; Wagner, M.; Jessen, F.; Weyerer, S.; Werle, J.; Wiese, B.; Lühmann, D.; Posselt, T.; König, H.H.; et al. Impact of coronary heart disease on cognitive decline in Alzheimer's disease: A prospective longitudinal cohort study in primary care. *Br. J. Gen. Pract.* **2017**, *67*, e111–e117. [CrossRef]